Enhancement in solar hydrogen generation efficiency using InGaN photoelectrode after surface roughening treatment with nano-sized Ni mask*

Tao Tao(陶 涛)[a)b)], Zhi Ting(智 婷)[a)b)], Li Ming-Xue(李民雪)[b)c)], Xie Zi-Li(谢自力)[a)b)†], Zhang Rong(张 荣)[a)b)], Liu Bin(刘 斌)[a)b)], Li Yi(李 毅)[a)b)], Zhuang Zhe(庄 喆)[a)b)], Zhang Guo-Gang(张国刚)[a)b)], Jiang Fu-Long(蒋府龙)[a)b)], Chen Peng(陈 鹏)[a)b)], and Zheng You-Dou(郑有炓)[a)b)]

[a)] *National Laboratory of Solid Microstructures, Nanjing University, Nanjing* 210093, *China*

[b)] *Jiangsu Provincial Key Laboratory of Advanced Photonic and Electronic Materials, School of Electronic Science and Engineering, Nanjing National Laboratory of Microstructures, Nanjing University, Nanjing* 210093, *China*

[c)] *Ecomaterials and Renewable Energy Research Center (ERERC), Department of Physics, Nanjing University, Nanjing* 210093, *China*

(Received 20 February 2014; revised manuscript received 10 April 2014; published online 23 July 2014)

A significant enhancement in solar hydrogen generation efficiency has been achieved by inductive coupled etching (ICP) surface roughening treatment using nano-sized nickel mask. As much as 7 times improvement of photocurrent is demonstrated in comparison with a planar one fabricated from the same parent wafer. Under identical illumination conditions in HBr solution, the incident photon conversion efficiency (IPCE) shows an enhancement with a factor of 3, which even exceed 54% at 400 nm wavelength. We believe the enhancement is attributed to several facts including improvement in absorption, reacting area, carrier localization and carrier lifetime.

Keywords: photoelectrolysis, InGaN photoelectrode, surface roughening, hydrogen generation

PACS: 62.23.st, 84.60.jt, 81.07.–b **DOI:** 10.1088/1674-1056/23/9/096203

1. Introduction

Clean hydrogen generation has been attracting increasing attention due to its environment friendly and unlimited resource property. However, at present, more than 95% hydrogen are still generated from fossil fuels and biomass.[1] Hydrogen generation via photoelectrolysis provides a promising solution to reduce carbon footprint as well as solving energy crisis.[2] Thus, numerous materials have been studied as photoelectrode.[3–6] Among them, InGaN epilayer is one of the most promising candidate for application due to its adjustable direct band gap perfectly matching the solar spectrum and stability in acidic/alkaline solution under sun light.[7–10] So far, some efforts have been done including nano-rod structure, electrochemical treatment, and so on.[11–14] There are still not enough research in InGaN-based photoelectrode.

In this paper, we demonstrate significant enhancement in hydrogen generation efficiency by employing surface roughening process on InGaN film with self-assembled nickel mask. The incident photon conversion efficiency (IPCE) of InGaN/GaN film is enhanced by a factor of 3, which is attributed to several factors. Moreover, time-dependence test of photocurrents shows a good resistance to corrosion in HBr solution after the roughening process.

2. Experimental details

The InGaN epi-wafer was grown on *c*-sapphire (0001) substrate by metal-organic chemical vapor-phase deposition (MOCVD) with a vertical gas-flow growth chamber (Thomas Swan 3x2″ CCS). The source precursors for Ga, In, and N were Trimethyl-gallium (TMGa), Trimethyl-indium (TMIn), and ammonia (NH_3), respectively. The N_2 or H_2 was used as carrier gas during the deposition. A 2.5-μm-thick silicon-doped n-type GaN buffer layer was firstly deposited, followed by a 250-nm-thick InGaN layer. 5-nm-thick Ni mask was deposited on the InGaN epi-layer and rapid thermal process (RTP) was applied to form nano-sized particles. After that, the sample was roughened by utilizing a standard inductive coupled plasma etching (ICP).[15] The etch depth was set as 50 nm, leaving 200-nm-thick InGaN layer untouched. Due to the poor metal-semiconductor contact of un-doped InGaN film, a part of area was etched down to n-GaN layer using ICP etch and photolithography techniques, where standard alloy of Ti/Al/Ni/Au (50 nm/100 nm/50 nm/100 nm) was deposited on the n-GaN layer in order to form ohmic n-contact. This is to some degree similar to the fabrication of the III-nitride based light emitting diodes (LEDs).[12] After being cleaned by acetone and deionized water, the photoelectrochemical prop-

*Project supported by the Special Funds for Major State Basic Research Project of China (Grant Nos. 2011CB301900, 2012CB619304, and 2010CB327504), the Hi-tech Research Project of China (Grant No. 2011AA03A103), the National Nature Science Foundation of China (Grant Nos. 60990311, 61274003, 60936004, and 61176063), the Program for New Century Excellent Talents in University of China (Grant No. NCET-11-0229), the Natural Science Foundation of Jiangsu Province of China (Grant No. BK2011010), the Funds of Key Laboratory of China (Grant No. 9140C140102120C14), and the Research Funds from NJU-Yangzhou Institute of Opto-electronics of China.

†Corresponding author. E-mail: xzl@nju.edu.cn

© 2014 Chinese Physical Society and IOP Publishing Ltd

erties of such samples were measured by a conventional three-electrode cell using an electrochemical analyzer (CHI-633C, Shanghai Chenhua). A 500-W xenon lamp was employed as a light source. The InGaN epi-wafer, a Pt wire, and a saturated calomel electrode (SCE) were used as working, counter and reference electrodes, respectively. Aqueous 1 M HBr solution was employed as an electrolyte because of its better stability. To prevent the GaN buffer layer from being excited and confirm all photocurrent comes from InGaN layer, a 390-nm cutoff filter was employed.

3. Results and discussion

Figure 1 shows the typical scanning electron microscope (SEM) images of InGaN electrode samples (plane-view image of origin sample in Fig. 1(a), with nano-sized nickel mask image in Fig. 1(b) and image of roughened sample with an angle of 45° in Fig. 1(c)). In Fig. 1(a), the surface of origin sample exhibit mountain-like and trench-like structure, which is common in InGaN epi-layer grown by MOCVD.[7,16,17] InGaN epi-layer grown on thick GaN template is usually under compressive strained state, which leads to the formation of stress driven surface undulations as shown in Fig. 1(a).[18] Figure 1(b) shows the surface of samples with self-assembled Ni mask after rapid thermal process.[12,15] The average nickel mask diameter is around 15 nm. Interestingly, the size and location of nano-sized Ni mask is closely associated with the morphology of InGaN alloys layer. It can be found most Ni particles locate at the slope or top of mounts, which is attributed to the self-organized mechanism. It selectively leaves the defects and valleys uncovered. After ICP roughening treatment being applied and residual Ni particles being removed, the sample surface is transformed into something similar to Karst land feature. Figure 1(c) shows the surface structure of such feature. The roughness of surface is clearly improved compared to the origin one in Fig. 1(a). Based on atomic force microscope (AFM) measurement, the average roughness is increased from 16.5 nm to around 40 nm. The root mean square (RMS) rises from 20 nm to 49 nm.

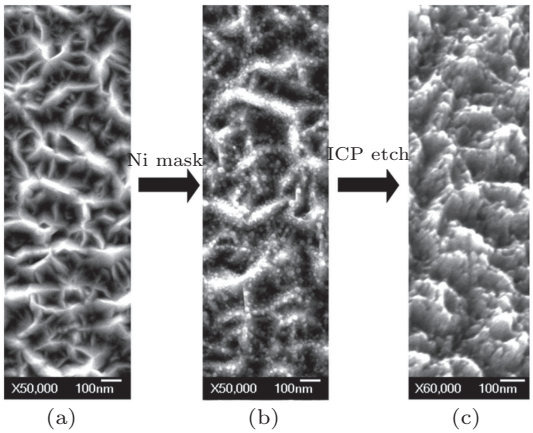


Fig. 1. Typical scanning electron microscope (SEM) images of InGaN electrode samples. (a) Image of sample surface before roughening, (b) image of sample with nickel mask, and (c) image of sample after surface roughening treatment with an angle of 45°.

The PL spectra of InGaN photoelectrode samples were measured with excitation of a 325-nm He-Cd laser, performed by a Reinshaw micro-PL system with laser spot size of about 5 μm. Figure 2 shows the PL spectra measured at room temperature, where the dominate peak at 440 nm corresponds to the near band edge emission of InGaN layer. The broad lower peak is believed to be the defects-related emission of GaN buffer layer.[19,20] From the PL spectra, the band gap energy of InGaN layer is calculated to be 2.82 eV. Inset indicates the reciprocal space mapping (RSM) of the asymmetric $(1\bar{1}05)$ InGaN/GaN sample conducted by PANalytical X'Pert Pro MRD triple-axis X-ray diffraction system. The upper contour represents the reflection of GaN layer, while the other two indicate the InGaN epi-layer. The center of the lower contour is close to that perpendicular align of the $(1\bar{1}05)$ GaN, labeled by a vertical black dashed line. Meanwhile, another one locates at that of fully relaxed states, labeled by the sideling black dashed line. According to previous reports,[21,22] the In content can be calculated as $x = 0.14$ and a degree of relaxation $R = 100\%$, while another corresponds to $x = 0.16$ and $R \sim 25\%$. Taking the strain state into consideration,[22,23] the energy gap of this ternary alloy is estimated by[24]

$$E_g^{(\mathrm{InGaN})} = xE_g^{(\mathrm{InN})} + (1-x)E_g^{(\mathrm{GaN})} - bx(1-x), \qquad (1)$$

where E_g and x are the bandgap of semiconductor and the In composition, respectively, and b is the bowing parameter. The energy gap of InGaN layer in this study is estimated to be about 2.85 eV, which agrees with the PL spectra above.

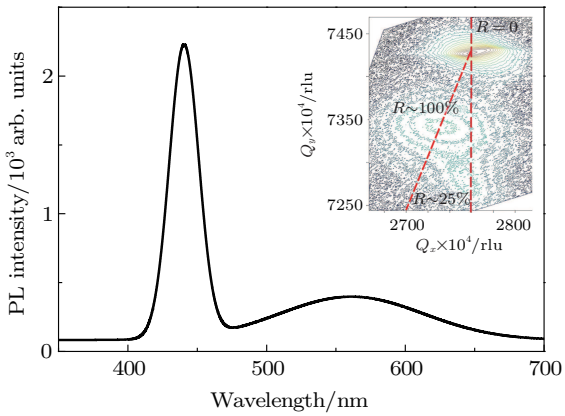


Fig. 2. (color online) The PL spectra of the InGaN epi-layer measured at room temperature. Inset: $(1\bar{1}05)$ RSMs for InGaN/GaN samples. The diffraction intensities are plotted in contours as a function of the components Q_y and Q_x of the reciprocal lattice vector relative to the direction normal and parallel to the sample surface (in units of $\sim 10000 \times 4\pi/\lambda$). The vertical dashed line implies the fully strained state of InGaN layer, while the sideling dashed line indicates the relaxed states.

The photocurrent of InGaN sample was investigated in 1 M HBr aqueous solution under $\lambda > 390$ nm illumination (in

Fig. 3). A 500-W xenon lamp was employed as light source. To prevent the GaN buffer layer from being excited and confirm that all photocurrent comes from InGaN layer, a 390-nm cutoff filter was employed. Dotted curve indicates the photocurrent of roughened sample with a lock-in amplifier, while the solid one represents that of origin sample. Obviously, as high as almost 7 times enhancement can be seen in Fig. 3, as well as even lower dark current. In order to further verify the beneficial effects of surface roughening process, incident photon conversion efficiency (IPCE) was obtained under the light with different wavelengths filtered by monochrome filters (shown in the inset of Fig. 3). The light intensity was measured with a photometer (Newport, 840-C). The IPCE of origin sample is around 16% at the wavelength of 400 nm, which is equal to some other literatures.[11,24] Interestingly, the IPCE of roughened sample reaches an encouraging value as much as 54%. More than 3 times enhancement has been acquired, which provides a vision of bringing InGaN-based hydrogen generation into practice.

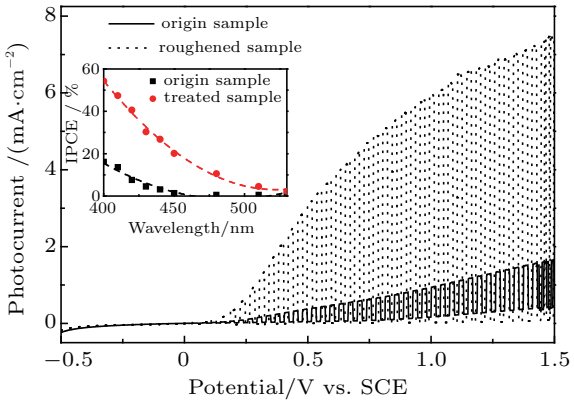


Fig. 3. (color online) Photocurrent density potential at InGaN electrode in 1M HBr solution under $\lambda > 390$ nm illumination with and without surface treatment. Inset: IPCE of InGaN electrode before and after the treatment; the potential is 1 V vs. SCE.

Such great improvement can be attributed to the following several factors: i) as shown in Fig. 1, such nano-sized Ni mask with a diameter of 20 nm and an average distance of 30 nm provides a massive increase in total surface area with a factor of about 3.61 compared to that of the origin feature. Therefore, light absorption is greatly enhanced, providing more photon-generated carriers in the active zone. On the other hand, it also increases the interface between water molecules and InGaN alloys, which benefits the electrochemical reaction speed shown in following equations:

$$\text{Semiconductor} + h\nu \rightarrow \text{e}^- + h^+, \tag{2}$$

$$\text{e}^- + \text{H}^+ \rightarrow 1/2\text{H}_2, \tag{3}$$

$$2h^+ + \text{H}_2\text{O} \rightarrow \text{O}_2 + 2\text{H}^+. \tag{4}$$

ii) Rough surface offers a kind of localization effect for photon-generated carriers, which raises the proportion of carriers involved in photoelectrical reaction. Originally, a large amount of carriers would move to non-radiative centers, bringing down the efficiency of photoelectrolysis. Because the density of threading dislocations in GaN-based epilayers is around 10^8–10^{10} cm^{-2}, which means that there are 1 to 100 non-radiative centers within every micron square.[7,19] The diffusion length of carriers can be above 200 nm.[25] Since the distance between carriers and surface is shortened by surface roughening, photon-generated carriers can reach the interface between InGaN layer and water molecules easier. It gains more carriers to participate in water splitting. iii) Once being fabricated down to nano size, so-called surface band bending takes in, the separation of the photon-generated electron–hole pairs was enhanced, resulting in longer recombination lifetimes. The performance of InGaN electrode relies on longer carrier lifetime.[14] iv) Slopes of mounts and trenches are covered by Ni mask, which provides a protection during the surface roughening, leaving InGaN layer beneath with good crystal quality. While, gullies are diminished or removed after roughening, where exist dislocations and defects. Thus, it also explains that lower dark current is achieved after surface roughening process, which is highly related to defects and threading dislocations.

The chronoamperometry (i–t) of InGaN electrode in 1 M HBr aqueous solution after the surface roughening process under illumination over wavelength of 390 nm was measured and shown in Fig. 4. The photocurrent is almost constant during a long time illumination (2500 s), which indicates the strong stability of InGaN electrode in acidic solution even after ICP etching.[26]

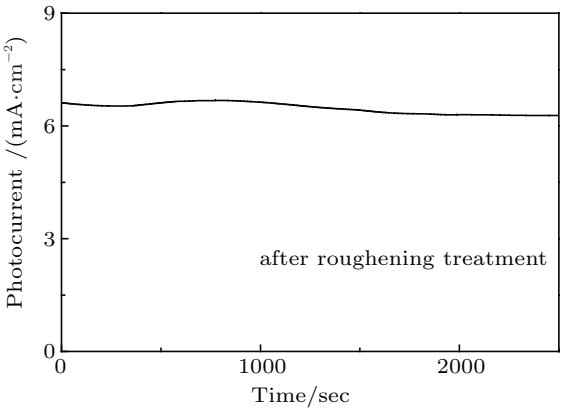


Fig. 4. Chronoamperometry (i–t) at InGaN electrode in 1 M HBr solution under $\lambda > 390$ nm illumination after the surface roughening treatment. The potential is 1 V vs. SCE.

4. Conclusions

In summary, the surface of 250-nm-thick InGaN epi-layer is roughened by the ICP etching with nano-sized Ni mask on top. Subsequently, photoelectrolysis of roughened InGaN electrode is studied. It is found that the photocurrent and the IPCE of such electrode increase almost 7 times and 3 times

after the roughening process, which are attributed to several factors including improved absorption, increased reacting interface, carrier localization, longer carrier lifetime, and selective etching. More than 54% IPCE is acquired under 400 nm wavelength condition and strong corrosion resistance is also demonstrated. It provides a promising route to achieve solar hydrogen generation with high efficiency.

References

[1] Holladay J D, Hu J, King D L and Wang Y 2009 *Catalysis Today* **139** 244

[2] Yilanci A, Dincer I and Ozturk H K 2009 *Progress in Energy and Combustion Science* **35** 231

[3] Feng X, LaTempa T J, Basham J I, Mor G K, Varghese O K and Grimes C A 2010 *Nano Lett.* **10** 948

[4] Wang H, Lindgren T, He J, Hagfeldt A and Lindquist S E 2000 *J. Phys. Chem. B* **104** 5686

[5] Ono M, Fujii K, Ito T, Iwaki Y, Hirako A, Yao T and Ohkawa K 2007 *J. Chem. Phys.* **126** 054708

[6] Usui S, Kikawa S, Kobayashi N, Yamamoto J, Ban Y and Matsumoto K 2008 *Jpn J. Appl. Phys.* **47** 8793

[7] Yıldız A, Öztürk M K, Bosi M, Özçelik S and Kasap M 2009 *Chin. Phys. B* **18** 4007

[8] Lai W, Zhao W, Hao Z B and Yi L 2011 *Chin. Phys. Lett.* **28** 57301

[9] Lu P Y, Ma Z G, Su S C, Zhang L, Chen H, Jia H Q, Jiang Y, Qian W N, Wang G, Lu T P and He M 2013 *Chin. Phys. B* **22** 106803

[10] Zhao B J, Chen X, Ren Z W, Tong J H, Wang X F, Li D W, Zhuo X J, Zhang J, Yi H X and Li S T 2013 *Chin. Phys. B* **22** 088401

[11] Li M X, Luo W J, Liu B, Zhao X, Li Z S, Chen D J, Yu T, Xie Z L, Zhang R and Zou Z G 2011 *Appl. Phys. Lett.* **99** 112108

[12] Benton J, Bai J and Wang T 2013 *Appl. Phys. Lett.* **102** 173905

[13] AlOtaibi B, Nguyen H P T, Zhao S, Kibria M G, Fan S and Mi Z 2013 *Nano Lett.* **13** 4356

[14] Yang J, Zhao D G, Jiang D S, Liu Z S, Chen P, Li L, Wu L L, Le L C, Li X J, He X G, Wang H, Zhu J J, Zhang S M, Zhang B S and Yang H 2013 *Chin. Phys. B* **22** 098801

[15] Wan T T, Ye Z Q, Tao T, Xie Z L, Zhang R, Liu B, Xiu X Q, Yi L, Han P, Shi Y and Zheng Y D 2013 *Chin. Phys. B* **22** 88102

[16] Massabuau F C P, Sahonta S L, Trinh-Xuan L, Rhode S, Puchtler T J, Kappers M J, Humphreys C J and Oliver R A 2012 *Appl. Phys. Lett.* **101** 212107

[17] Ting S M, Ramer J C, Florescu D I, Merai V N, Albert B E, Parekh A, Lee D S, Lu D, Christini D V, Liu L and Armour E A 2003 *J. Appl. Phys.* **94** 1461

[18] Bruckbauer J, Edwards P R, Wang T and Martin R W 2011 *Appl. Phys. Lett.* **98** 141908

[19] Reshchikov M A and Morkoç H 2005 *J. Appl. Phys.* **97** 061301

[20] Ogino T and Aoki M 1980 *JPN J. Appl. Phys.* **19** 2395

[21] Wilsch B, Jahn U, Jenichen B, Lahnemann J, Grahn H T, Wang H and Yang H 2013 *Appl. Phys. Lett.* **102** 052109

[22] Moram M A and Vickers M E 2009 *Reports on Progress in Physics* **72** 036502

[23] Wu J, Walukiewicz W, Yu K M, Ager J W, Haller E E, Lu H and Schaff W J 2002 *Appl. Phys. Lett.* **80** 4741

[24] Liu B, Luo W J, Zhang R, Zou Z G, Xie Z L, Li Z S, Chen D J, Xiu X Q, Han P and Zheng Y D 2010 *Physica Status Solidi* **7** 1817

[25] Liuolia V, Marcinkevičius S, Lin Y D, Ohta H, DenBaars S P and Nakamura S 2010 *J. Appl. Phys.* **108** 023101

[26] Aryal K, Pantha B N, Li J, Lin J Y and Jiang H X 2010 *Appl. Phys. Lett.* **96** 052110